Heliyon 8 (2022) e10010

Contents lists available at ScienceDirect

Heliyon

journal homepage: www.cell.com/heliyon

Research article

Biosynthesis and antibacterial activity of silver nanoparticles using *Flos Sophorae Immaturus* extract

Zhong Cheng [a,b], ShanWen Tang [a,b], Jing Feng [a,b], Yu Wu [a,b,c,*]

[a] Department of Pharmacy, School of Pharmacy and Bioengineering, Chongqing University of Technology, Chongqing, 400054, China
[b] Chongqing Key Laboratory of Medicinal Chemistry & Molecular Pharmacology, Chongqing, 400054, China
[c] Department of Biomedical Materials Science, Third Military Medical University, Chongqing, 400038, China

ARTICLE INFO

Keywords:
Biosynthesis
Flos sophorae immaturus extract
Ag NPs
Nanotechnology
Bacteria
Antibacterial activity

ABSTRACT

The current study proposes a green synthesis method for silver nanoparticles (Ag NPs) using various concentrations of *Flos Sophorae Immaturus* extract as reducing and capping agents. The UV-Visible (UV-Vis) spectroscopy, X-ray Diffraction (XRD), Fourier Transform Infrared spectroscopy (FTIR), X-ray Photoelectron Spectroscopy (XPS), Dynamic Light Scattering (DLS) and Transmission Electron Microscopy (TEM) were used to characterize resulting brown nanopowder. The as-prepared Ag NPs had a high negative zeta potential value of ~ -38 mv, indicating the existence of electrostatic stabilization. The average sizes of ~27.8 nm, 28.5 nm, 34.3 nm and 36.5 nm were measured by TEM. Moreover, FTIR and XPS analyses validated the production and chemical composition of Ag NPs from silver nitrate. The antibacterial activity of Ag NPs was examined against *E. coli*, *P. aeruginosa*, and *S. aureus* using agar well diffusion and the minimum inhibitory concentration (MIC) method. The antibacterial activity of the as-prepared Ag NPs from 4 mL extract was excellent against *E. coli*, *P. aeruginosa*, and *S. aureus* and the MIC values were 31.250, 15.625, and 31.250 mg/L, respectively. Based on these results, this study proposes a practical approach for the synthesis of Ag NPs in the industry and medical fields.

1. Introduction

Multidrug-Resistant (MDR) infections of microorganism pathogens are becoming common due to the abuse of antimicrobials and natural selection in the environment. The MDR bacteria genetically and biochemically overcome antibiotics stress, posing major challenges for the treatment of hospital and community-acquired infectious diseases [1, 2, 3]. For instance, *E. coli*, *P. aeruginosa* and *S. aureus* are resistant to methicillin and penicillin and can cause serious risks of burns, urinary tract infections, and post-operative infections [4, 5, 6, 7]. Therefore, it is necessary to explore novel viable strategies against MDR pathogens for public health. Presently, the introduction of nanomaterials with unique properties, particularly metal nanoparticles, offers new prospects to eradicate and treat the aforementioned diseases.

Among the metal nanoparticles, Ag NPs have been widely used as antibacterial agents because of their broad-spectrum bactericidal properties against some common bacteria and low minimum inhibitory concentration (MIC) [8, 9]. In general, reducing agents and surfactants are frequently used during the chemical synthesis of Ag NPs, to reduce silver ions and control the growth of Ag NPs [10]. However, due to the involvement of these toxic compounds, chemical methods suffer various deficiencies. Therefore, it is crucial to make more effort to explore environmentally friendly methods for preparing Ag NPs.

Researchers are increasingly interested in biosynthetic methods since they avoid toxic chemicals and involve simple steps [11, 12]. In comparison to other chemical methods, biosynthetic methods can synthesize Ag NPs with controlled size and shape without using hazardous substances [9, 13]. Fungi, algae, bacteria, and plants, among others, may currently synthesize Ag NPs [14]. The plant extract has been a better choice among the different bio-tools owing to their abundant components that can act as reducing as well as stabilizing agents. *Thymus algeriensis*, *Jasminum subtriplinerve Blume*, and *Cinnamomum camphora* leaf extracts were used to biosynthesize Ag NPs with higher antibacterial activity [15, 16, 17]. Furthermore, the *Flos Sophorae Immaturus* extract contains numerous polyhydroxy flavonoids with strong antioxidant activity, which can act as reducing agents in the production of Ag NPs [18].

The objective of this study is to develop a simple approach to the biosynthesis of Ag NPs. We successfully synthesized Ag NPs of different sizes using varying amounts of *Flos Sophorae Immaturus* extract as reducing and capping agents. A series of characterization techniques

* Corresponding author.
E-mail address: dushulang51@cqut.edu.cn (Y. Wu).

https://doi.org/10.1016/j.heliyon.2022.e10010
Received 17 February 2022; Received in revised form 24 March 2022; Accepted 15 July 2022

including Ultraviolet-Visible (UV-Vis) spectroscopy, X-ray Diffraction (XRD), X-ray Photoelectron Spectroscopy (XPS), Fourier Transform Infrared spectroscopy (FTIR) and Transmission Electron Microscopy (TEM), were used to validate the properties of the biosynthesized Ag NPs. The agar well diffusion and MIC methods were used to evaluate the antibacterial activities of Ag NPs against *E. coli*, *P. aeruginosa*, and *S. aureus*. This study will provide a cost-effective and environmentally friendly approach to the synthesis of Ag NPs.

2. Materials and methods

2.1. Materials and chemicals

Flos Sophorae Immaturus was obtained from the traditional Chinese medicine store, Chongqing. Rutin (>98.0%) was provided by Gelipu Biotechnology Co. Ltd, Chengdu. Dimethyl sulfoxide (C_2H_6OS, DMSO) was obtained from Titan Technology Co. Ltd, Shanghai. Methanol (HPLC grade) was supplied by Honeywell Burdick & Jackson trading, Ltd, Shanghai. Calcium hydroxide ($Ca(OH)_2$) was supplied from Damao Chemical Reagent Factory, Tianjin. Sodium tetraborate pentahydrate ($NaBH_4{\cdot}5H_2O$) and silver nitrate were purchased from Kelong Chemical Reagent Factory, Chengdu. Agar was obtained from Chron Chemicals, Ltd, Chengdu. Peptone, Beef extract, and Yeast extract were procured from Aoboxing bio-tech Co. Ltd, Beijing. *E. coli*, *P. aeruginosa,* and *S. aureus* bacterial strains were stored in our laboratory. Throughout the experiments, double distilled water was used. All the reagents were used without further purification.

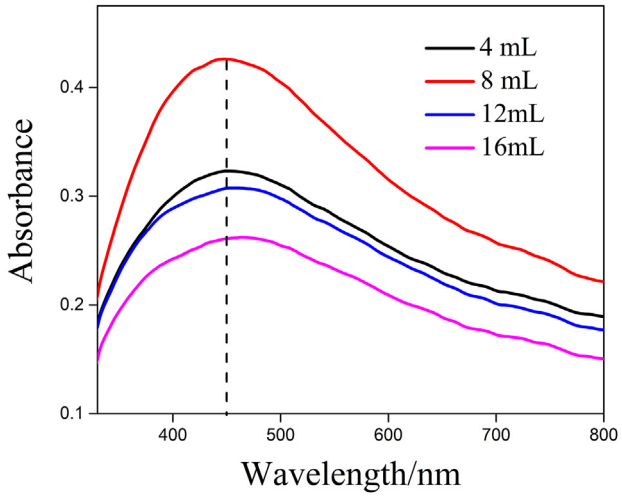

Figure 1. UV-Vis spectra of Ag NPs synthesized from different volumes of extract.

2.2. Preparation of Flos Sophorae Immaturus extract and HPLC analysis

The dried *Flos Sophorae Immaturus* were ground into a coarse powder. A ratio of 20 g: 200 mL between *Flos Sophorae Immaturus* dosage and freshly prepared 0.4% $NaBH_4$ solution was used. After 1 h of simmering, the pH of the mixture was adjusted to 8–9 with saturated $Ca(OH)_2$ solution. After cooling, the extract was vacuum filtered and stored at 4 °C for further use. The main ingredient of the extract was detected by High Performance Liquid Chromatography (HPLC). A reversed-phase column (Sinopak, 5 μm C18, 150 mm × 4.6 mm, Elite, Dalian, China) was used with an HPLC system (LC-20A, Shimadzu, Kyoto, Japan). The mobile phase was methanol: water (40: 60 v/v) with acetic acid (1%) using isocratic elution at 1.0 mL/min. Chromatograms were taken at 257 nm with a run time of 20 min.

2.3. Biosynthesis of Ag NPs

Different volumes of *Flos Sophorae Immaturus* extract (4, 8, 12, 16 mL) and 40 mL $AgNO_3$ solution (4 mM) were added to beakers, respectively. All reactions were performed at room temperature for 5 h in the dark. The production of Ag NPs was noticed as the colloidal solution turned to dark brown color. Subsequently, the samples were centrifuged at 10000 rpm for 3 min and the precipitate was dried in an oven.

2.4. Characterization of Ag NPs

UV-Vis spectroscopy, XRD, DLS, TEM, FTIR, and XPS were used to characterize the structure, morphology, and elemental composition of the as-prepared samples. Spectrophotometer UV 2600 (Tianmei Scientific Instrument Co. Ltd, China) was used to measure UV-Vis spectra of Ag NPs over a wavelength range of 330–800 nm. To investigate the crystallographic character of Ag NPs, XRD patterns were obtained in the 2θ range from 5° to 85° by an X-ray diffractometer (D8 ADVANCE, Bruker, Germany) using Cu Ka radiation (λ = 1.5406 Å). At room temperature, the Zeta potential of Ag NPs was measured by Brookhaven 90 Plus Particle Size Analyzer (Brookhaven Instruments Corporation, American). TEM (JEM2100, JEOL, Japan) was used to examine the morphology and size of Ag NPs at an accelerating voltage of 200 kV. The surface composition of Ag NPs was identified by FTIR (Spectrum Two, PerkinElmer, USA) in the range of 4000–400 cm^{-1} and XPS (ESCALAB 250Xi, Thermo-VG Scientific, USA) using Al-Ka (1486.6 eV) radiation.

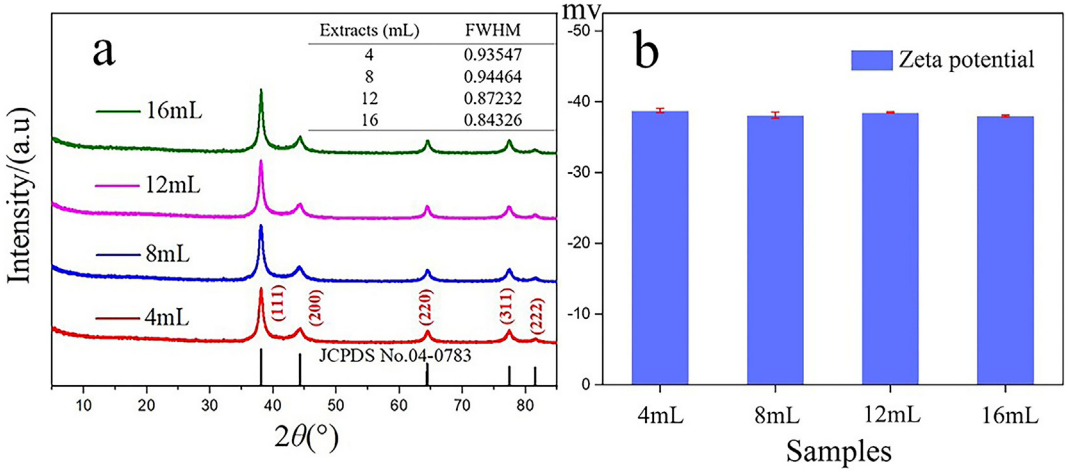

Figure 2. XRD patterns (a), Zeta potential values (b) of Ag NPs synthesized from different additional volumes of extract.

2.5. Antibacterial activity of Ag NPs

To examine the antibacterial activity of the as-prepared Ag NPs against *E. coli*, *P. aeruginosa*, and *S. aureus*, the agar well diffusion method was used to culture *E. coli* and *S. aureus* grew in Luria-Bertani (LB) nutrient solution and incubated at 37 °C for 6 h, whereas *P. aeruginosa* was grown in Nutrient Broth and incubated at 30 °C for 6 h. The bacteria were then diluted to a 5–8×10^7 colony-forming unit (CFU/mL) with sterilized water.

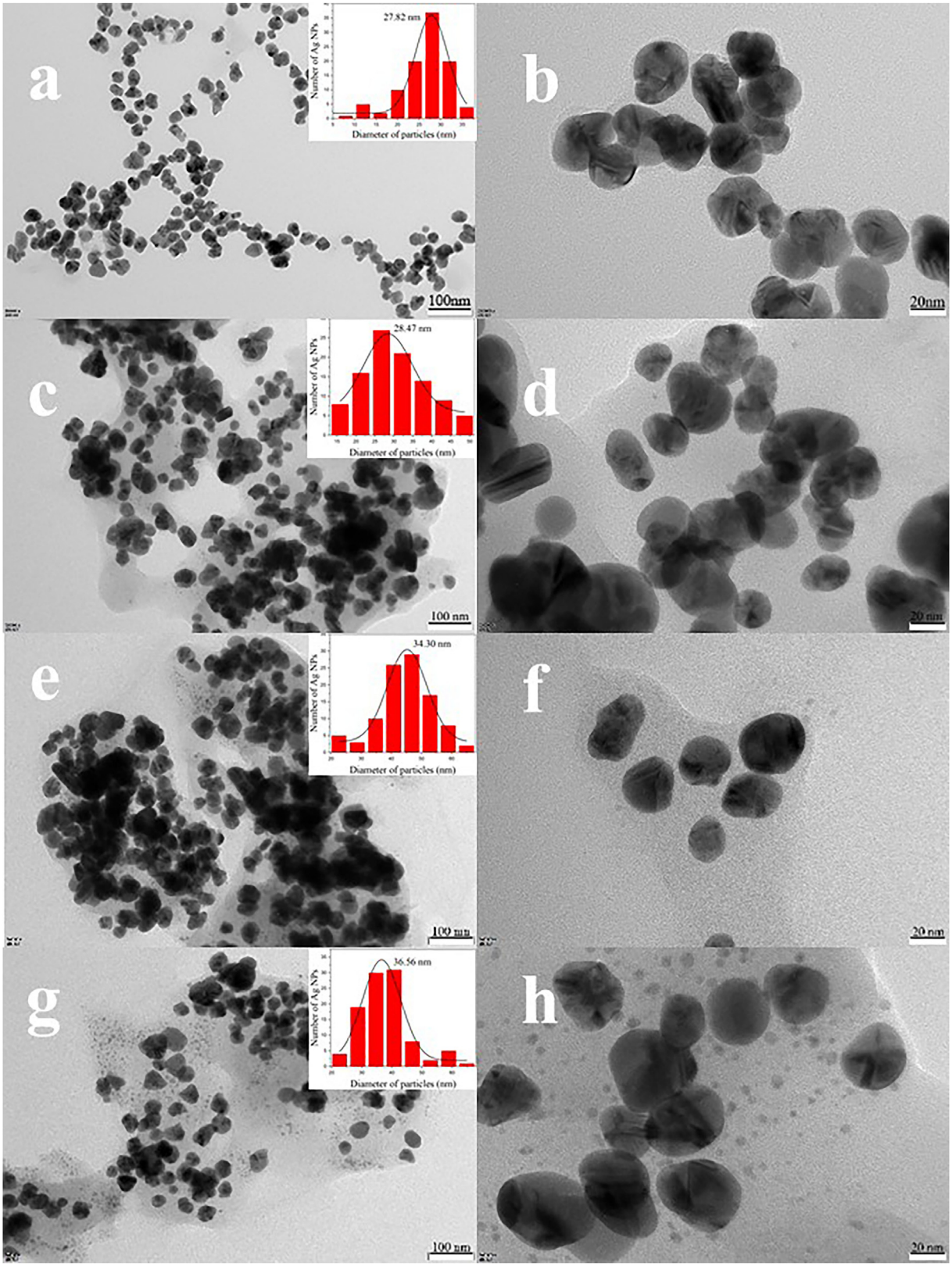

Figure 3. TEM images of Ag NPs synthesized by 4 mL (a, b), 8 mL (c, d), 12 mL (e, f), and 16 mL (g, h) extract, the insets are the histograms of the corresponding Ag particles size distribution, counts = 100.

The 100 μL bacterial suspensions (5–8 × 10^7 CFU/mL) of *E. coli* and *S. aureus* were pipetted and spread on the surface of Petri plates containing LB medium. Similarly, 100 μL bacterial suspensions (5–8 × 10^7 CFU/mL) of *P. aeruginosa* were swabbed on the surface of Petri plates containing Nutrient Agar Broth medium. Then, wells with 8.0 mm diameter were made on the plate, and 100 μL of Ag NPs solution (2 mg/mL) and 50% DMSO (negative control) were added to respective wells. After 12 h of incubation at 37 °C, the Zone of Inhibition (ZOI) was measured using a Vernier caliper. All the experiments were repeated 5 times independently, and the data were calculated as means ± SD.

The broth microdilution method was used to determine the minimum inhibitory concentration (MIC) [19]. Serial dilutions of Ag NPs were prepared using a broth medium. The 100 μL of various concentrations of Ag NPs (500–3.75 μg/mL) were transferred into 96-well microplates and then mixed with 10 μL of *E. coli*, *P. aeruginosa*, and *S. aureus* (5–8 × 10^5 CFU/mL) [20]. The mixed solutions were incubated at 37 °C for 16 h. Finally, UV-Vis spectroscopy was used to measure the absorbance of wells at 600 nm, and the OD600 measurement indicates the bacterial growth kinetics in a broth medium [21]. The MIC was considered to be the lowest concentration that inhibits visible bacterial growth, and all the experiments were done in triplicate.

3. Results and discussion

3.1. Characterization

UV-Vis spectroscopy was used to monitor the formation of Ag NPs from different amounts of extract (4, 8, 12, 16 mL). The single and strong peak around 450 nm shown in Figure 1 indicates the bioreduction of Ag^+ ions to Ag^0 by extract [22, 23]. Moreover, when the additional volume was more than 8 mL, the surface plasmon resonance (SPR) absorption peaks of Ag NPs showed a slight red-shift (from 450 to 465 nm), which can be ascribed to the increase in the size of Ag NPs [24]. It could be due to the interaction between capping molecules attached to the surface of particles and the secondary reduction process on the surface of the accomplished nuclei [25].

Figure 2a shows the XRD patterns of the synthesized Ag NPs. It displays five distinct diffraction peaks at 81.61°, 77.42°, 64.33°, 44.35°, and 38.10°, corresponding to the diffractions of (222) (311) (220) (200), and (111) lattice planes of face-centered cubic silver (JCPDS card No. 04–0783) [26]. The full width at half maximum (FWHM) of the (111) lattice plane was determined by MDI Jade 6.5 software. When the extract volume addition increased to 12 and 16 mL, FWHM become significantly narrower. This may be attributed to the increase in size of Ag NPs, which is consistent with the UV-Vis analysis [27].

The stability of Ag NPs was predicted by Zeta potential analysis. The zeta potential values of the as-prepared Ag NPs are displayed in Figure 2b, and it ranges from -37.89 ± 0.12 mV to -38.77 ± 0.31 mV, confirming the negative-charged groups on the surface of Ag NPs. The negatively charged surface aids in preventing the aggregation of Ag NPs and controlling the shape and size of Ag NPs [22].

The size and morphology of nanoparticles were characterized by TEM analysis. As illustrated in Figure 3, the images show the agglomeration of small grains and some dispersed nanoparticles, which corresponds with

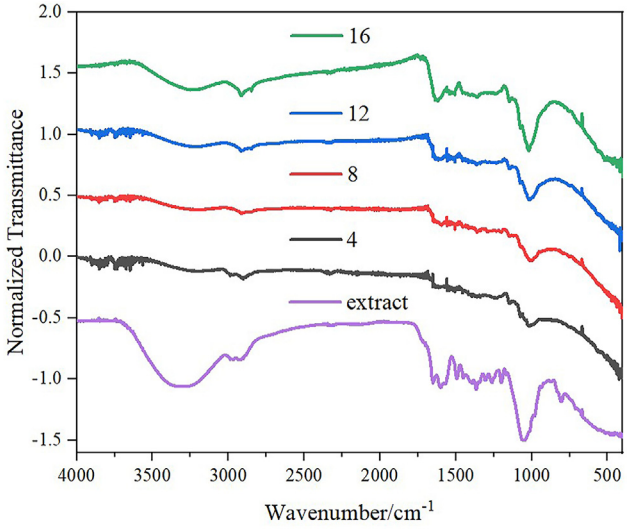

Figure 5. FTIR spectra of extract (purple line) and Ag NPs synthesized by adding 4 mL (black line), 8 mL (red line), 12 mL (blue line), and 16 mL (green line) extract.

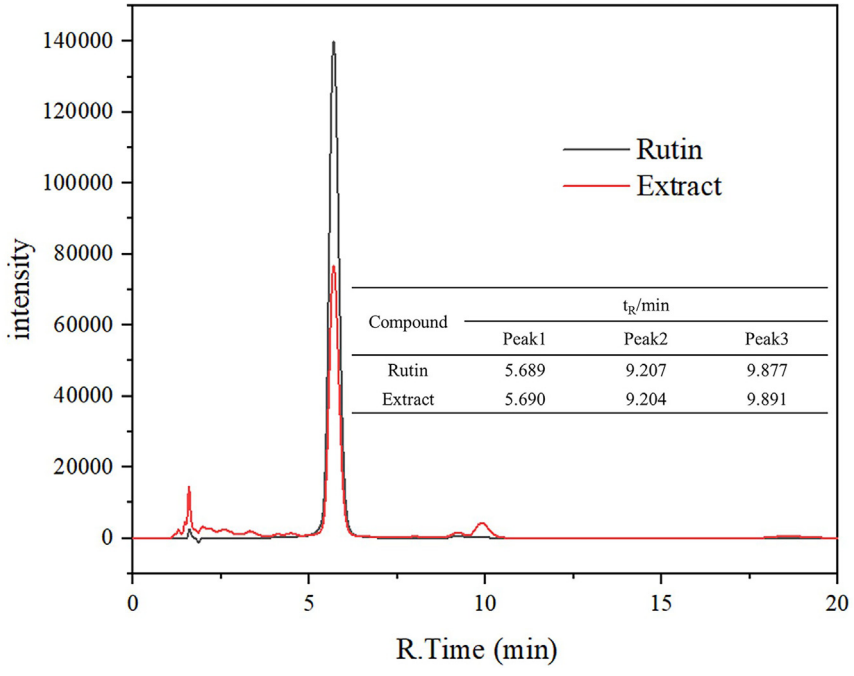

Compound	t_R/min		
	Peak1	Peak2	Peak3
Rutin	5.689	9.207	9.877
Extract	5.690	9.204	9.891

Figure 4. Chromatograms of rutin and extract.

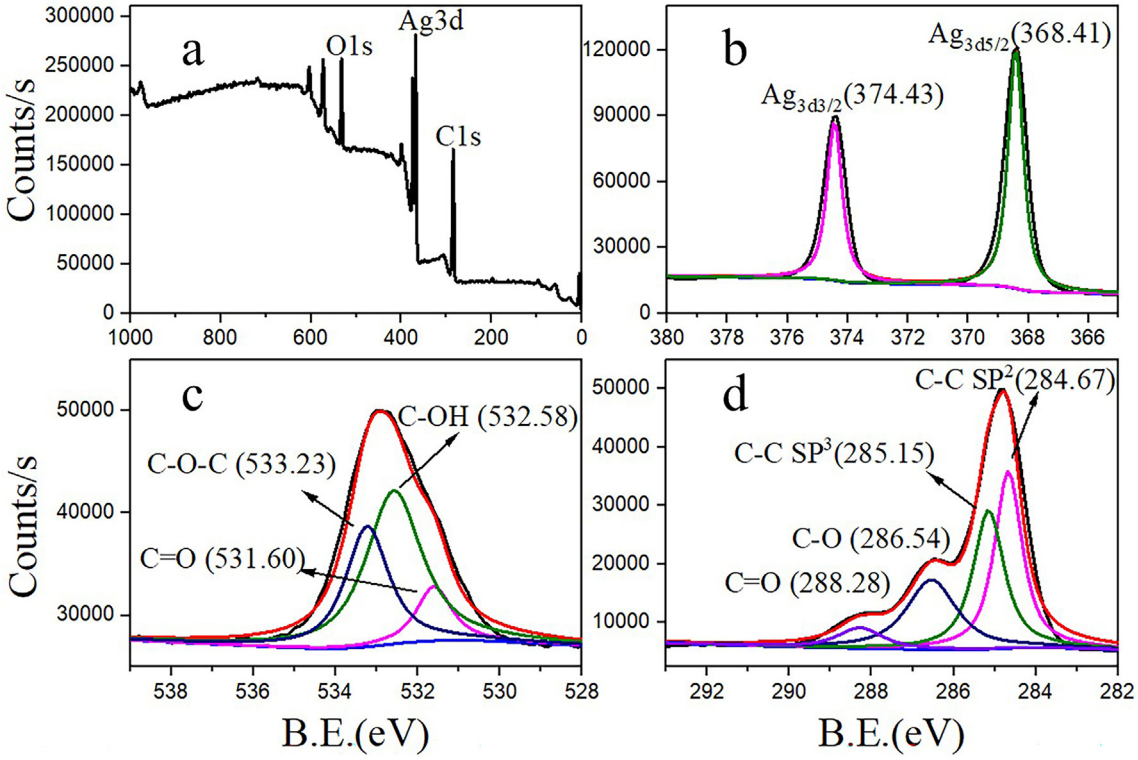

Figure 6. XPS spectrum of Ag NPs synthesized from 4 mL extract. Survey scan of Ag NPs (a), XPS high-resolution spectrum of Ag3d region (b), O1s region (c) and C1s region (d).

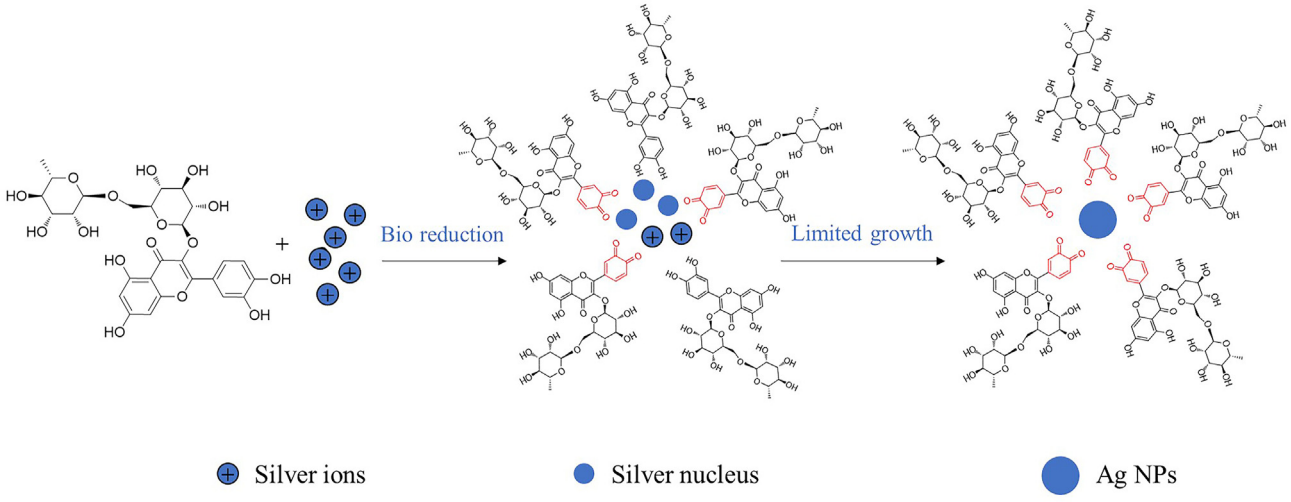

Figure 7. The mechanism for the greed synthesis of Ag NPs using *Flos Sophorae Immaturus* extract.

the previous findings [28]. The average size of the synthesized Ag NPs from 4 mL, 8 mL, 12 mL, and 16 mL extracts are ~27.8 nm, 28.5 nm, 34.3 nm and 36.5 nm, respectively. The particle size gradually increased with an increasing volume of the extract, confirming the response observed in the SPR band, as shown in Figure 1.

The rutin was discovered to be the primary component in *Flos Sophorae Immaturus* [29]. In this study, HPLC was used to identify rutin in *Flos Sophorae Immaturus* extract. Chromatograms of rutin and extract are presented in Figure 4. At the same chromatographic condition, the retention time of the main component in the extract is consistent with rutin. Therefore, rutin was the main component of the *Flos Sophorae Immaturus* extract.

Figure 5 shows the FTIR spectra of *Flos Sophorae Immaturus* extract and the green synthesized Ag NPs by adding different volumes of extract. According to the spectra of Ag NPs, the peak at 3269 cm^{-1}, 2910 cm^{-1}, 1628 cm^{-1} and 1009 cm^{-1} correspond to O–H stretching, C–H stretching vibration of CH_2, C=O stretching, and C–O–C stretching, which consistent with the spectrum of *Flos Sophorae Immaturus* extract. The FTIR spectra suggest that rutin in extract acts as a capping and reducing agent.

Table 1. Antibacterial activity of Ag NPs synthesized from different volumes of extract.

Pathogenic microorganisms	Zone of Inhibition (mm)			
	4 mL	8 mL	12 mL	16 mL
E. coli	16.28 ± 0.55	15.56 ± 0.91	15.42 ± 0.88	14.06 ± 0.83
S. aureus	16.28 ± 0.77	13.82 ± 1.25	13.44 ± 1.34	12.28 ± 0.74
P. aeruginosa	14.42 ± 0.08	12.98 ± 0.61	13.06 ± 0.94	12.76 ± 0.94

The detailed chemical states of the Ag NPs synthesized from 4 mL extract were further analyzed by XPS. Some clear peaks are assigned to Ag3d, C1s, and O1s as illustrated in Figure 6a. The high-resolution spectra of Ag3d are shown in Figure 6b, and the binding energies of $Ag3d_{3/2}$ and $Ag3d_{5/2}$ are 374.43 and 368.41 eV, respectively. The difference of ~6.0 eV between $Ag3d_{3/2}$ and $Ag3d_{5/2}$ indicates the formation of Ag NPs [30, 31]. Additionally, the high-resolution O1s and C1s spectra indicate the presence of biocompounds derived from the extract. The high-resolution O1s spectrum (Figure 6c) displays a broad peak deconvoluted into three subpeaks at ~531.60, ~532.58, and ~533.23 eV corresponding to C=O, C–OH, and C–O–C [32, 33]. These functional groups are derived from the phytochemicals of *Flos Sophorae Immaturus* extract. The C1s spectrum of the synthesized Ag NPs is deconvoluted into four subpeaks, with binding energies of C=C (sp2 carbon), C–C (sp3 carbon), C–O and C=O are ~284.67, ~285.15, ~286.54, and ~288.28 eV, respectively (Figure 6d) [34, 35].

3.2. Mechanism for the green synthesis of Ag NPs

The green synthesized Ag NPs can reduce the use of organic solvents as well as avoid the production of toxic waste. Rutin is the primary component in *Flos Sophorae Immaturus* extract as per HPLC and FTIR studies, and it acts as a capping and reducing agent during the green synthesis of Ag NPs. Previous research found that the –OH groups in flavonoids may reduce silver ions to Ag NPs [36, 37]. Figure 7 depicts a schematic of the proposed mechanism for the Ag NPs synthesis by *Flos Sophorae Immaturus* extract. Firstly, the tautomeric transformation of flavonoids from enols to ketones can release active hydrogen atoms, which are responsible for the reduction of silver ions to silver nuclei. Subsequently, cumulative reactions on these nuclei lead to the formation of larger Ag NPs.

3.3. Antibacterial activity

The agar well diffusion method was used to assess the antibacterial activity of the synthesized Ag NPs against gram-negative (*E. coli* and *P. aeruginosa*) and gram-positive (*S. aureus*) bacteria. The Zone of Inhibition (ZOI) for Ag NPs at the concentration of 2 mg/mL is summarized in Table 1 and Figure 8. The maximum ZOI was observed in the synthesized Ag NPs from 4 mL extract, with the inhibition zone diameters of 16.28 ± 0.55 mm, 16.28 ± 0.77 mm and 14.42 ± 0.08 mm against *E. coli*, *S. aureus,* and *P. aeruginosa*, respectively. Furthermore, the synthesized Ag NPs from 16 mL extract has the lowest antibacterial activity against *E. coli*, *S. aureus,* and *P. aeruginosa*, with ZOI ~14.06 ± 0.83 mm, 12.28 ± 0.74 mm and 12.76 ± 0.94 mm, respectively. The results show that the synthesized Ag NPs from various amounts of extract had a significant inhibitory effect on both Gram-negative and Gram-positive bacteria. The antibacterial activity of Ag NPs is closely related to the particle size, with smaller Ag NPs having higher activity than larger ones.

The MIC of the synthesized Ag NPs from 4 mL extract is defined as the minimum concentration of Ag NPs that inhibits the growth of bacteria. The broth microdilution method was used to calculate the MIC for Ag NPs against these three tested bacteria (Figure 8 inset) in this study. The MIC for *P. aeruginosa* was found to be 15.625 mg/L, whereas the MIC for *E. coli* and *S. aureus* was 31.250 mg/L. A comparison of the antibacterial activity of the green synthesized Ag NPs with other antibacterial Ag NPs is summarized in Table 2. The Ag NPs synthesized by *Flos Sophorae Immaturus* extract appear to have a higher bactericidal effect against *E. coli*, *S. aureus*, and *P. aeruginosa*.

The antibacterial mechanism of biosynthesized Ag NPs has not been fully understood. Recent studies have reported the generalized mechanisms such as (i) the interactions between Ag^+ and sulfur-/phosphate-rich proteins in the cell membrane and wall can enhance the permeability leading to breakage of the bacterial cells, and (ii) Ag^+ penetrates the bacterial cells and accelerate the generation of ROS, causing cell membrane disruption and DNA modification [26, 40, 41].

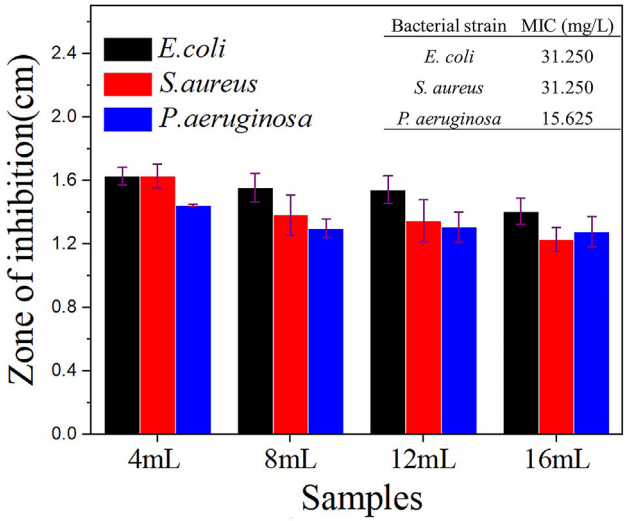

Figure 8. The ZOI of the synthesized Ag NPs against *E. coli*, *S. aureus*, and *P. aeruginosa* (Errors bars represent the standard deviation of the mean, n = 5).

Table 2. Comparison of MIC of Ag NPs synthesized from different plants against different pathogens.

Plants	Diameter (nm)	Pathogen	MIC (μg/mL)	References
Cacumen platycladi	60	*E. coli*	40	[38]
		S. aureus	80	
Decaspermum parviflorum	8–15	*E. coli*	31.25	[22]
		S. aureus	62.50	
		p. aeruginosa	15.62	
Xanthostemon chrysanthus	6–25	*E. coli*	31.25	
		S. aureus	15.62	
		p. aeruginosa	62.50	
Syzygium campanulatum	24–55	*E. coli*	31.25	
		S. aureus	62.50	
		p. aeruginosa	31.25	
Carya illinoinensis leaf	20.34	*S. aureus*	128	[39]
		L. monocytogenes	64	
		E. coli	16	
		p. aeruginosa	32	
Flos Sophorae Immaturus	27.8	*E. coli*	31.250	This work
		S. aureus	31.250	
		p. aeruginosa	15.625	

4. Conclusion

We proposed a cost-effective and environmentally friendly method for the synthesis of Ag NPs in this study using various amounts of *Flos Sophorae Immaturus* extract as effective reducing and stabilizing agents. The synthesized Ag NPs were characterized by multiple techniques. The formation of Ag NPs was confirmed by UV-Vis spectroscopy, XRD and XPS. The morphology of nanoparticles is generally spherical, with an average size ranging from 25 to 40 nm, and the high negative zeta potential values indicated that Ag NPs have good stability. The resulting Ag NPs also demonstrated excellent antibacterial activity against gram-negative (*E. coli* and *P. aeruginosa*) and gram-positive (*S. aureus*) bacteria, with antibacterial activities increasing as the size of the nanoparticles decreased. These biosynthesized Ag NPs have a broad spectrum of antimicrobial activities for bacteria and have the potential to be good antibacterial agents in multiple fields.

Declarations

Author contribution statement

Zhong Cheng: Conceived and designed the experiments; Performed the experiments; Analyzed and interpreted the data; Wrote the paper.

Shanwen Tang: Conceived and designed the experiments; Performed the experiments.

Jing Feng: Performed the experiments.

Yu Wu: Conceived and designed the experiments; Analyzed and interpreted the data; Contributed reagents, materials, analysis tools or data; Wrote the paper.

Funding statement

This work was supported by the Scientific Research Foundation of Chongqing University of Technology (Grants No. 2019ZD14), the Science and Technology Research Project of Chongqing Education Commission (Grants No. KJQN201801115), and the Natural Science Foundation of Chongqing (No. cstc2021jcyj-bshX0084).

Data availability statement

Data included in article/supplementary material/referenced in article.

Declaration of interests statement

The authors declare no conflict of interest.

Additional information

No additional information is available for this paper.

References

[1] M. Alavi, N. Karimi, Biosynthesis of Ag and Cu NPs by secondary metabolites of usnic acid and thymol with biological macromolecules aggregation and antibacterial activities against multi drug resistant (MDR) bacteria, Int. J. Biol. Macromol. 128 (2019) 893–901.

[2] M. Masi, M. Réfregiers, K.M. Pos, J.M. Pagès, Mechanisms of envelope permeability and antibiotic influx and efflux in gram-negative bacteria, Nat. Microbiol. 2 (2017), 17001.

[3] M. Baym, L.K. Stone, R. Kishony, Multidrug evolutionary strategies to reverse antibiotic resistance, Science 351 (2016) 6268.

[4] A. Khan, W.R. Miller, C.A. Arias, Mechanisms of antimicrobial resistance among hospital-associated pathogens, Expert Rev. Anti Infect. Ther. 16 (4) (2018) 269–287.

[5] J. Song, A. Walters, D. Berridge, A. Akbari, M. Evans, R.A. Lyons, Risk factors for Escherichia coli bacteraemia: a population-based case-control study, The. Lancet. 390 (2017) S85.

[6] T. Mestrovic, S. Ljubin-Sternak, Molecular mechanisms of chlamydia trachomatis resistance to antimicrobial drugs, Front. Biosci. 23 (2018) 656–670.

[7] L.K. Ruddaraju, S.V.N. Pammi, G.S. Guntuku, V.S. Padavala, V.R.M. Kolapalli, A review on anti-bacterials to combat resistance: from ancient era of plants and metals to present and future perspectives of green nano technological combinations, Asian J. Pharm. Sci. 15 (1) (2020) 42–59.

[8] A.N. Brown, K. Smith, T.A. Samuels, J. Lu, S.O. Obare, M.E. Scott, Nanoparticles functionalized with ampicillin destroy multiple-antibiotic-resistant isolates of Pseudomonas aeruginosa and enterobacter aerogenes and methicillin-resistant staphylococcus aureus, Appl. Environ. Microbiol. 78 (2012) 2768–2774.

[9] N. Ahmad, S. Sharma, V.N. Singh, S.F. Shamsi, A. Fatma, B.R. Mehta, Biosynthesis of silver nanoparticles from desmodium triflorum: a novel approach towards weed utilization, Biotechnol. Res. Int. 2011 (2011), 454090.

[10] Z.Q. Cheng, Z.W. Li, J.H. Xu, R. Yao, Z.L. Li, S. Liang, G.L. Cheng, Y.H. Zhou, X. Luo, J. Zhong, Morphology-controlled fabrication of large-scale dendritic silver nanostructures for catalysis and SERS applications, Nanoscale Res. Lett. 14 (1) (2019) 1–7.

[11] S. Iravani, Green synthesis of metal nanoparticles using plants, Green Chem. 13 (2011) 2638–2650.

[12] V.V. Makarov, A.J. Love, O.V. Sinitsyna, S.S. Makarova, I.V. Yaminsky, M.E. Taliansky, N.O. Kalinina, "Green" nanotechnologies: synthesis of metal nanoparticles using plants, Acta. Nat. 6 (2014) 35–44.

[13] A. Mahanty, S. Mishra, R. Bosu, U. Maurya, S.P. Netam, B. Sarkar, Phytoextract-synthesized silver nanoparticles inhibit bacterial fish pathogen aeromonas hydrophila, Indian J. Microbiol. 53 (2013) 438–446.

[14] S. Jadoun, R. Arif, N.K. Jangid, R.K. Meena, Green synthesis of nanoparticles using plant extract: a review, Environ. Chem. Lett. 19 (1) (2021) 355–374.

[15] M. Beljilali, K. Mekhissi, Y. Khane, W. Chaibi, L. Belarbi, S. Bousalem, Antibacterial and antifungal efficacy of silver nanoparticles biosynthesized using leaf extract of thymus algeriensis, J. Inorg. Organomet. Polym. Mater. 20 (2019) 2126–2133.

[16] P.A. Nguyen, H.P. Phan, T. Dang-Bao, V.M. Nguyen, N.L. Duong, X.T. Huynh, P.P.T. Vo, T.Y.L. Pham, T.N.Q. Bui, T. Nguyen, Sunlight irradiation assisted green synthesis, characteristics and antibacterial activity of silver nanoparticles using the leaf extract of Jasminum subtriplinerve Blume, J. Plant Biochem. Biotechnol. 31 (2022) 202–205.

[17] W. Li, F. Qu, Y.B. Chen, Y.F. Sun, J.J. Zhang, G.Y. Xie, Q.X. You, H.Y. Xu, Antimicrobial activity of sliver nanoparticles synthesized by the leaf extract of Cinnamomum camphora, Biochem. Eng. J. 172 (2021), 108050.

[18] Q.H. Li, Z.Q. Luan, J.K. Wang, The chemical components, Chinese medicine processing and pharmacological effect on sophora flower bud, Acta. Chin. Med. Pharmaco. 45 (2017) 112–116.

[19] M. Oves, M. Aslam, M.A. Rauf, S. Qayyum, H.A. Qari, M.S. Khan, M.Z. Alam, S. Tabrez, A. Pugazhendhi, I.M.I. Ismail, Antimicrobial and anticancer activities of silver nanoparticles synthesized from the root hair extract of phoenix dactylifera, Mater. Sci. Eng. C 89 (2018) 429–443.

[20] M. Elshikh, S. Ahmed, S. Funston, P. Dunlop, M. McGaw, R. Marchant, I.M. Banat, Resazurin-based 96-well plate microdilution method for the determination of minimum inhibitory concentration of biosurfactants, Biotechnol. Lett. 38 (6) (2016) 1015–1019.

[21] Z.H. Ni, X.X. Gu, Y. He, Z.H. Wang, X.Y. Zou, Y.B. Zhao, L. Sun, Synthesis of silver nanoparticle-decorated hydroxyapatite (HA@Ag) poriferous nanocomposites and the study of their antibacterial activities, RSC Adv. 8 (73) (2018) 41722–41730.

[22] S. Paosen, J. Saising, A.W. Septama, S.P. Voravuthikunchai, Green synthesis of silver nanoparticles using plants from Myrtaceae family and characterization of their antibacterial activity, Mater. Lett. 209 (2017) 201–206.

[23] M.D. Balakumaran, R. Ramachandran, P. Balashanmugam, D.J. Mukeshkumar, P.T. Kalaichelvan, Mycosynthesis of silver and gold nanoparticles: optimization, characterization and antimicrobial activity against human pathogens, Microbiol. Res. 182 (2016) 8–20.

[24] Y.P. Wu, Y. Yang, Z.J. Zhang, Z.H. Wang, Y.B. Zhao, L. Sun, A facile method to prepare size-tunable silver nanoparticles and its antibacterial mechanism, Adv. Powder Technol. 29 (2) (2018) 407–415.

[25] N. Nagar, S. Jain, P. Kachhawah, V. Devra, J. Korean, Synthesis and characterization of silver nanoparticles via green route, Chem. Eng. 33 (10) (2016) 2990–2997.

[26] S. Devanesan, M.S. AlSalhi, Green synthesis of silver nanoparticles using the flower extract of Abelmoschus esculentus for cytotoxicity and antimicrobial studies, Int. J. Nanomed. 16 (2021) 3343–3356.

[27] M. Gomathi, A. Prakasam, P.V. Rajkumar, Green synthesis, characterization and antibacterial activity of silver nanoparticles using amorphophallus paeoniifolius leaf extract, J. Cluster Sci. 30 (4) (2019) 995–1001.

[28] A. Rautela, J. Rani, M. Debnath, Green synthesis of silver nanoparticles from Tectona grandis seeds extract: characterization and mechanism of antimicrobial action on different microorganisms, J Anal. Sci. Technol. 10 (5) (2019).

[29] J.L. Huang, W.J. Xie, Extraction of rutin from *Flos Sophorae Immaturus* with an aqueous 1-butyl-3-methylimidazolium chloride solution, Anal. Sci. 26 (3) (2010) 383.

[30] M.J. Shu, F.J. He, Z.H. Li, X.Z. Zhu, Y.J. Ma, Z.H. Zhou, Z. Yang, F. Gao, M. Zeng, Biosynthesis and antibacterial activity of silver nanoparticles using yeast extract as reducing and capping agents, Nanoscale Res. Lett. 15 (1) (2020) 14.

[31] P.U. Rani, P. Rajasekharreddy, Green synthesis of silver-protein (core-shell) nanoparticles using piper betel L. leaf extract and its ecotoxicological studies on Daphnia magna, Colloids. Surf. A. Physicochem. Eng. Aspects. 389 (2011) 188–194.

[32] G. Beamson, D. Briggs, High resolution monochromated X-ray photoelectron spectroscopy of organic polymers: a comparison between solid state data for organic polymers and gas phase data for small molecules, Mol. Phys. 76 (4) (1992) 919–936.

[33] M. Mani, J.H. Chang, G.A. Dhanesh, V.D. Kayal, S. Pavithra, K. Mohanraj, B. Mohanbabu, B. Babu, S. Balachandran, S. Kumaresan, Environmental and biomedical applications of AgNPs synthesized using the aqueous extract of solanum surattense leaf, Inorg. Chem. Commun. 121 (2020), 108228.

[34] C.S.A. Caires, L.A.S. Farias, L.E. Gomes, B.P. Pinto, D.A. Gonçalves, L.F. Zagonel, V.A. Nascimento, D.C.B. Alves, I. Colbeck, C. Whitby, A.R.L. Caires, H. Wender, Effective killing of bacteria under blue-light irradiation promoted by green synthesized silver nanoparticles loaded on reduced graphene oxide sheets, Mater. Sci. Eng. C. Mater. Biol. Appl. 113 (2020), 110984.

[35] G.A. Bhaduri, R. Little, R.B. Khomane, S.U. Lokhande, B.D. Kulkarni, B.G. Mendis, L. Šiller, Green synthesis of silver nanoparticles using sunlight, J. Photochem. Photobiol. Chem. 258 (15) (2013) 1–9.

[36] S. Jain, M.S. Mehata, Medicinal Plant leaf extract and pure flavonoid mediated green synthesis of silver nanoparticles and their enhanced antibacterial property, Sci. Rep. 7 (2017) 1–13.

[37] F. Tasca, R. Antiochia, Biocide activity of green quercetin-mediated synthesized silver nanoparticles, Nanomaterials 10 (5) (2020) 909.

[38] X.Y. Huang, L. Chang, Y.G. Lu, Z.H. Li, Z.W. Kang, X.H. Zhang, M.H. Liu, D.P. Yang, Plant-mediated synthesis of dual-functional Eggshell/Ag nanocomposites towards catalysis and antibacterial applications, Mat. Sci. Eng. C-Mater. 113 (2020), 111015.

[39] S.J.B. Dalir, H. Djahaniani, F. Nabati, M. Hekmati, Characterization and the evaluation of antimicrobial activities of silver nanoparticles biosynthesized from Carya illinoinensis leaf extract, Heliyon 6 (3) (2020), e03624.

[40] F. Abdelghaffar, M.G. Mahmoud, M.S. Asker, S.S. Mohamed, Facile green silver nanoparticles synthesis to promote the antibacterial activity of cellulosic fabric, J. Ind. Eng. Chem. 99 (25) (2021) 224–234.

[41] R. Krishnamoorthi, P.U. Mahalingam, B. Malaikozhundan, Edible mushroom extract engineered Ag NPs as safe antimicrobial and antioxidant agents with no significant cytotoxicity on human dermal fibroblast cells, Inorg. Chem. Commun. 139 (2022) 109362–109375.